© 2017 IJSRSET | Volume 3 | Issue 6 | Print ISSN: 2395-1990 | Online ISSN : 2394-4099
Themed Section: Engineering and Technology

Vibrational Assignments, Homo-Lumo, NLO, NBO, MEP, Mulliken's Charge and Thermodynamical Parameter Analyses of M-Xylene-Alpha, Alpha – DIOL

L. Bhuvaneswari[*,a], U. Sankar[b], S.MeenakshiSundar[c]

[a]Department of Physics, N.K.R.Government Arts College for women, Namakkal, India

[b]Department of Physics, Sri K.G.S. Arts College, Srivaikuntam, India

[c]Department of Physics, Sri Paramakalyani College, Alwarkurichi, India

ABSTRACT

Xylene is used as a feedstock in the production of petrol. It is also found in small proportions in gasoline and jet fuel. It is extensively used as a thinner and solvent in paints, varnishes, adhesives and inks. A xylene mixture can be used to thin lacquers (a black resinous substance used a natural varnish) when slower drying is desired. Xylene is often used as a solvent in pesticides products. The majority (more than 90 percent) of mixed xylene isomers is used for blending into petrol and gasoline, and the rest in different solvent applications for the printing industry, pharmaceuticals, perfumes, fabricated items and pesticide formulations, to name a few. Xylene is also used in the preparation of individual isomers, which are often used in making certain types of plastics. By combining all these facts into account, the present investigation has been aimed to investigate the vibrational spectra of M-xylene-alpha, alpha –diol (MXAAD). Investigations have also been carried out to identify the HOMO-LUMO energy gap, NLO property (First-Hyperpolarizability), Molecular electrostatic potential (MESP), chemical hardness, chemical potential and delocalization activity of the electron clouds in the optimized molecular structure. All these investigations have been done on the basis of the optimized geometry by using density functional theory (DFT) B3LYP/6-31+G and B3LYP/6-311+G level.

Keywords: FT-IR, FT-Raman, NLO, NBO, Thermodynamical property

I. INTRODUCTION

Xylene is a clear, colorless, sweet-smelling solution of three aromatic hydrocarbon isomers produced from crude oil through a process called alkylation. Xylene consists of three distinct isomers: paraxylene, orthoxylene and metaxylene. Xylene is both naturally occurring and man made, and is widely used as a solvent in the leather, rubber and printing industries. Other applications of xylene include chemical intermediates, and high-motor and aviation gasoline blending agents. Xylene is also used in breathing devices (inhalers) for administering artificial respiration because of its intoxicating properties. In small doses, it produces euphoria and disinhibition, but it also causes dizziness and hallucinations. Xylene is a raw material in the production of a monomer (a simple compound with molecules that join together to form polymers) called terephthalic acid. Terephthalic acid is used in the manufacture of polymers (naturally occurring or synthetic compounds consisting of large molecules). It is a good cleaning agent for silicon wafers and steel. It is also used to sterilize many substances. Xylene is used as a feedstock in the production of petrol. It is also found in small proportions in gasoline and jet fuel. It is extensively used as a thinner and solvent in paints, varnishes, adhesives and inks. A xylene mixture can be used to thin lacquers (a black resinous substance used a natural varnish) when slower drying is desired. Xylene is often used as a solvent in pesticides products. The majority (more than 90 percent) of mixed xylene isomers is used for blending into petrol and gasoline,

and the rest in different solvent applications for the printing industry, pharmaceuticals, perfumes, fabricated items and pesticide formulations, to name a few. Xylene is also used in the preparation of individual isomers, which are often used in making certain types of plastics. By combining all these facts into account, the present investigation has been aimed to investigate the vibrational spectra of M-xylene-alpha, alpha diol (MXAAD). Investigations have also been carried out to identify the HOMO-LUMO energy gap, NLO property (First-Hyperpolarizability), Molecular electrostatic potential (MESP), chemical hardness, chemical potential and delocalization activity of the electron clouds in the optimized molecular structure. All these investigations have been done on the basis of the optimized geometry by using density functional theory (DFT) B3LYP/6-31+G and B3LYP/6-311+G level.

II. EXPERIMENTAL DETAILS

The compound under investigation namely m-xylene-alpha,alpha diol (MXAAD) is purchased from Lancaster Chemical Company, UK which is of spectroscopic grade and hence used for recording the spectra as such without any further purification.

The FT-IR spectrum of the compound is recorded in PERKIN-ELMER, FT-IR model 1600 spectrophotometer in the region 4000-400 cm^{-1} using KBr pellet technique. The spectral resolution is ± 1 cm^{-1}. The FT-Raman spectrum of this compound is also recorded in the region 3500-50 cm^{-1} by using BRUKER IFS 66V model with FRA 106 Raman module equipped with Nd:YAG laser source operating at 1.064 μm line width 200 mW power. The spectra are recorded with scanning speed 30 cm^{-1} min^{-1} of spectral width 1 cm^{-1}. The frequencies of all sharp bands are accurate to ± 1 cm^{-1}.

III. QUANTUM CHEMICAL CALCULATION

The entire quantum chemical calculations have been performed at DFT (B3LYP) [69-70] method with 6-31+G and 6-311+G basis sets using the GAUSSIAN 09W program [1]. The optimized structural parameters have been evaluated for the calculation of vibrational frequencies at DFT theory and a small to large basis set by assuming C_1 point group symmetry. As a result, the unscaled frequencies, are obtained. In order to fit the theoretical wavenumber to the experimental, the scaling factors have been introduced using a least square optimization to the experimental data. The total energy distribution (TED) are computed from quantum chemically calculated vibrational frequencies using MOLVIB [2,3] program. GAUSSVIEW program [4] has been considered to get visual animation and also for the verification of the normal modes assignment. The HOMO-LUMO analysis has been carried out to explain the charge transfer within the molecule. The chemical hardness and chemical potential are also calculated using the Highest Occupied Molecular Orbital (HOMO) and Lowest Unoccupied Molecular Orbital (LUMO) energies. NBO analysis has been performed on MXAAD in order to elucidate the intermolecular hydrogen bonding, intermolecular charge transfer (ICT), rehybridization and delocalization of electron density.

IV. RESULTS AND DISCUSSION

4.1. Molecular Geometry

The molecular structure of m-Xylene alpha, alpha-Diol is shown in Fig. 7.1. The global minimum energy obtained by DFT structure optimization are found to be -461.30296 Hartrees and -461.19786 Hartrees by using B3LYP/6-311+G and B3LYP/6-31+G method and basis set respectively. The optimized bond length, bond angles and dihedral angles of MXAAD which are calculated using DFT (B3LYP) method with same basis sets are shown in Table 1.

The detailed description of vibrational modes can be given by means of normal coordinate analysis. The theoretically calculated DFT force fields are transformed to this set of vibrational coordinates and used in all subsequent calculations.

4.2. Vibrational Spectra

The title compound belongs to C_1 point group symmetry. For C_1 symmetry there would not be any revelant distribution. The molecule consists of 20 atoms and it leads to 54 normal modes of vibrations. These modes are found to be IR and Raman active suggesting that the molecule possesses a non-centro symmetric structure which recommends MXAAD for non-linear optical applications.

The detailed vibrational assignments of fundamental modes of MXAAD along with the calculated IR and Raman frequencies and normal mode description is presented in Table 7.2. The small difference between the experimental and calculated vibrational modes is observed. This discrepancy can come from the formation of intermolecular hydrogen bonding. Also, we note that the experimental results belongs to the solid phase and the theoretical calculations belongs to the gaseous phase. The FT-IR and FT-Raman spectra of MXAAD are shown in Fig.2&3, respectively.

O-H Vibrations

Hydrogen bonding alerts the frequencies of the stretching and bending vibrations. The O-H stretching bands move to lower frequencies usually with increase intensity and band broadening in the hydrogen bonded species. Hydrogen bonding present in five or six member ring system would reduce the O-H stretching bands to 3200-3550 cm^{-1} region [5]. The O-H in-plane-bending vibration in general, lies in the region 1150-1250 cm^{-1} and is not much affected due to hydrogen bonding unlike the stretching and out-of-plane deformation frequencies. The O-H out-of-plane deformation vibration lies in the region 290-320 cm^{-1} for free O-H [6]. In MXAAD, the FT-IR band appeared at 3220 cm^{-1} is assigned to O-H stretching vibration. The in-plane and out-of-plane bending vibration of hydroxyl group identified at 1239 and 710 cm^{-1} for MXAAD in FT-IR spectrum.

C-H Vibrations

The heterocyclic aromatic compound and its derivatives are structurally very close to benzene. The C-H stretching vibration [6, 7-8] of aromatic and heteroaromatic structure occur in the region 3000-3100 cm^{-1}. This permits the ready identification of the structure. Accordingly, in the present investigation the C-H stretching vibrations of MXAAD are observed at 3199 cm^{-1} in the FT-IR spectrum and at 3150, 3062 and 2951 cm^{-1} in the FT-Raman spectrum. The in-plane and out-of-plane bending vibrations of C-H group are found well within the characteristic region [9-10] and are presented in Table 2.

C-C Vibrations

Generally, the C-C stretching vibrations in aromatic compound form the band in the region of 1430-1650 cm^{-1} [11-12]. According to Socrates [13], the presence of conjugate substituent such as C=C causes a heavy doublet formation around the region 1625-1575 cm^{-1}. The bands between 1400-1650 cm^{-1} are assigned to carbon-carbon vibration [14]. In the present investigation the FT-IR bands observed at 1601, 1481, 1460, 1448, 1370 and 1312 cm^{-1} and FT-Raman bands observed at 1511, 1463, and 1455 cm^{-1} are assigned to carbon-carbon stretching vibrations. The C-C in-plane and out-of-plane vibrations are observed and listed in Table 2.

C-O Vibrations

The interaction of carbonyl group with other groups present in the system does not produce such a drastic and characteristic changes in the frequency of C-O stretch as did by interaction of O-H stretch. In the present study, the FT-IR band observed at 1288 cm^{-1} have been assigned for C-O stretching vibration. The in-plane and out-of-plane bending vibration of C-O group are also found well within the characteristic region [15] and listed in Table 2.

V. FRONTIER MOLECULAR ORBITAL ANALYSIS

Molecular orbitals (HOMO and LUMO) and their properties such as energy are very useful for physicists and chemists and are very important parameters for quantum chemistry. This is also used by the frontier electron density for predicting the most reactive position in π-electron systems and also explains several types of reaction in conjugated system [16]. The conjugated molecules are characterized by a small highest occupied molecular orbital-lowest unoccupied molecular orbital (HOMO-LUMO) separation, which is the result of a significant degree of intra molecular charge transfer from the end-capping electron-donor groups to the efficient electron-acceptor groups through π-conjugated path [17]. Both the highest occupied molecular orbital and lowest unoccupied molecular orbital are the main orbital which takes part in chemical stability [18]. The HOMO represents the ability to donate an electron, LUMO represents the ability to obtain an electron. The HOMO and LUMO energy calculated by B3LYP/6-311+G method is shown below. This electronic absorption corresponds to the transition from the ground to the first excited state and is mainly described by one electron excitation from the highest occupied molecular orbital to the lowest unoccupied molecular orbital. While the energy of the HOMO is directly related to the ionization potential, LUMO energy is directly related to the electron affinity. Energy difference between HOMO and LUMO orbital is called as energy gap which is an important stability for structures [19] and is calculated as

HOMO energy	=	-7.12357 eV
LUMO energy	=	-0.98364 eV
HOMO-LUMO energy gap	=	6.13993 eV

Recently, the energy gap between HOMO and LUMO has been used to prove the bioactivity from intra-molecular charge transfer [20-21]. The plots of HOMO and LUMO are shown in Fig 4.

VI. MOLECULAR ELECTROSTATIC POTENTIAL (MESP)

In order to grasp the molecular interactions, the molecular electrostatic potentials (MESP) are used. Recently, the MESP have been used for interpreting and predicting relative reactivities sites for electrophilic and nucleophilic attack, investigation of biological recognition, hydrogen bonding interactions, studies of molecular cluster, crystal behaviour, the correlation and prediction of a wide range of macroscopic properties [22,23]. Since MESP is related to total charge distribution of the molecule and it provides the correlations between the molecular properties such as partial charges, dipole moments, electronegativity and chemical reactivity of molecules.

In this study, the electrostatic potentials at the surface are represented by different colours. Red colour parts represent the regions of negative electrostatic potential while blue ones represent regions of positive electrostatic potential. Additionally, green colour parts represent the regions of zero potential. The negative regions of V(r) potential are related to electrophilic reactivity, while the positive ones are related to nucleophilic reactivity. MESP of MXAAD are calculated from optimized molecular structure by using B3LYP/6-311+G level and 3D plots of MESP are given in Fig 5.

VII. FIRST HYPERPOLARIZABILITY ANALYSIS

The first hyperpolarizability (β_0) of this novel molecular system of MXAAD is calculated using B3LYP/6-311+G basis set, based on the finite-field approach. In the presence of an applied electric field, the energy of a system is a function of the electric field. First hyperpolarizability is a third rank tensor that can be described by a $3 \times 3 \times 3$ matrix. The 27 components of the 3D matrix can be reduced to 10 components due to the Kleinman symmetry [24]. It can be given in the lower tetrahedral format. It is obvious that the lower part of the $3 \times 3 \times 3$ matrices is a tetrahedral. The components of β are defined as the coefficients in the Taylor series expansion of the energy in the external electric field. When the external electric field is weak and homogeneous, the expansion becomes as follow:

$$\beta_0 = \left(\beta_x^2 + \beta_y^2 + \beta_z^2\right)^{1/2}$$

where $\beta_x = \beta_{xxx} + \beta_{xyy} + \beta_{xzz}$

$\beta_y = \beta_{yyy} + \beta_{xxy} + \beta_{yzz}$ ... (1)

$\beta_z = \beta_{zzz} + \beta_{xxz} + \beta_{yyz}$

The components of polarizability and the first hyperpolarizability of MXAAD can be seen in Table 7.3. The first hyperpolarizability of MXAAD is 1.0041×10^{-30}

esu which is 2 times greater than those of urea (β of urea is 0.3728×10^{-30} esu). The calculated value of first hyperpolarizability shows that MXAAD might have the NLO properties.

VIII. MULLIKEN POPULATION ANALYSIS

The total atomic charges of m-xylene-alpha, alpha–Diol obtained by Mulliken's population analysis with B3LYP in different basis sets are listed in Table 4. From the result it is clear that the substitution CH_2 atoms in the aromatic ring leads to a redistribution of electron density. The σ-electron withdrawing character of the hydrogen atom in MXAAD is demonstrated by the decrease of electron density. The atomic charges in the CH_2 group are almost identical. The Mulliken charge obtained from 6-311+G basis set shows that C_1, C_3, C_4, H_7, H_8, H_9, H_{10}, H_{12}, H_{13}, H_{15}, H_{17}, H_{18} and H_{20} atoms are more acidic due to more positive charge. The Mulliken plot of MXAAD is as shown in Fig 6.

IX. NBO ANALYSIS

The second order Fock matrix is carried out to evaluate the donor-acceptor interactions in the NBO analysis (25). The interaction result is a loss of occupancy from the localized NBO of the idealized Lewis structure into an empty non-Lewis orbital. For each donor (i) and acceptor (j), the stabilization energy $E^{(2)}$ associated with the delocalization $i \rightarrow j$ is estimated as

$$E^{(2)} = \Delta E_{ij} = q_i \frac{F(i,j)^2}{\varepsilon_j - \varepsilon_i} \quad \ldots (2)$$

where q_i is the donor orbital occupancy, ε_i and ε_j diagonal elements orbital energies and F(i, j) is the off diagonal NBO Fock matrix element.

Natural bond orbital analysis provides an efficient method for studying intra and intermolecular bonding and interaction among bonds, and also provides a convenient basis for investigating charge transfer or conjugative interaction in molecular systems. Some electron donor orbital, acceptor orbital and the interacting stabilization energy resulted from the second-order micro-disturbance theory are reported [26-27]. The larger the $E^{(2)}$ value, the more intensive is the interaction between electron donors and electron acceptors, i.e., the more donating tendency from electron donors to electron acceptors and the greater the extent of conjugation of the whole system. Delocalization of electron density between occupied Lewis-type (bond or lone pair) NBO orbitals and formally unoccupied (antibond or Rydgberg) non-Lewis NBO orbitals correspond to a stabilizing donar-accepter interaction. NBO analysis has been performed on the molecule at the B3LYP/6-311+G level in order to elucidate intra moelcular, rehybridization and delocalization of electron density within the molecule.

The intra-molecular interactions are formed by the orbital overlap between bonding (C-C), (C-H) and (C-O) and bonding orbital which results intramolecular charge transfer (ICT) causing stabilization of the system. These interactions are observed as increase in electron density (ED) in C-C, C-O anti bonding orbital that weakens the respective bonds.

The hyperconjugative interaction of the π (C_1-C_6), (C_2-C_3) and (C_4-C_5) enhanced conjugate with antibonding orbital of π* (C_4-C_5), (C_1-C_6) and (C_2-C_3) leads to strong delocalixation of 20.78, 22.51 and 22.24 kJ/mol, respectively and it was represented in Table 5.

X. THERMO DYNAMIC PROPERTIES

Several thermodynamic properties like heat capacity, zero point vibrational energy, entropy of the compound MXAAD have been obtained by density functional methods using 6-311+G and 6-31+G basis set calculations are presented in Table 7.6. The difference in the values calculated by both the methods is only marginal. The dipole moment of a bond depends on the differences in electro negativity between two atoms in the bond. The thermo dynamic functions like enthalpy(E), Heat Capacity (Cv) and entropy (s) of MXAAD at room temperature are also represented in Table 7 and the values of this thermodynamic function are represented in Fig 7.

XI. CONCLUSION

The present investigation thoroughly analyzes the vibrational spectra of m-xylene- alpha, alpha – diol. All the vibrational bands observed in the FT-IR and FT-Raman spectra of MXAAD are assigned to the various modes of vibration. The complete vibrational assignments of wave numbers are made on the basis of the total energy distribution (TED). The optimized geometrical parameters calculated at B3LYP/6-311+G basis set are slightly larger than those calculated at

B3LYP/6-311+G. HOMO and LUMO energy gap explains the eventual charge transfer interactions taking place within the molecule. Mulliken charges and dipole moment of m- xylene- alpha, alpha – diol are also discussed elaborately.

XII. REFERENCES

[1]. M.J. Frisch, G.W. Trucks, H.B. Schlegal, G.E. Scuseria, M.A. Robb,J.R. Cheesman, V.G. Zakrzewski, J.A. Montgomerg, Jr., R.E. Stratmann, J.C. Burant, S. Dapprich, J.M. Millam, A.D. Daniels, K.N. Kudin, M.C. Strain, O. Farkas, J. Tomasi, V. Barone, M. Cossi, R. Cammi, B. Mennucci, C. Pomelli, C. Adamo, S. Clifford, J. Ochterski, G.A. Petersson, P.Y. Ayala, Q. Cui, K. Morokuma, N. Rega, P. Salvador, J.J. Dannenberg, D.K. Malich, A.D. Rabuck, K. Raghavachari, J.B. Foresman, J. Cioslowski, J.V. Ortiz, A.G. Baboul, B.B. Stetanov, G. Liu, A. Liashenko, P. Piskorz, I. Komaromi, R. Gomperts, R.L. Martin, D.J. Fox, T. Keith, M.A. Al-Laham, C.Y. Peng, A. Nanayakkara, M. Challacombe, P.M.W. Gill, B. Johnson, W. Chen, M.W. Wong, J.L. Andres, C. Gonzalez, M. Head-Gordon, E.S. Replogle and J.A. Pople, GAUSSIAN 98, Revision A 11.4, Gaussian, Inc, Pittsburgh PA, 2009.

[2]. T. Sundius, J. Mol. Struct., 218 (1990) 321 (a) T, Sundius, Vib. Spectrosc., 29 (2002) 89. (b) MOLVIB (V.7.0): Calculation of Hormonic Force Fields and Vibrational Modes of Molecules, QCPE program No. 807 (2002).

[3]. A. Frisch, A.B. Nielson, A.J. Holder, Gaussview Users Manual, Gaussian Inc, Pittsburgh PA, 2009.

[4]. D.N. Sathyanarayana, Vibrational Spectroscopy - Theory and Applications, seconded, New Age International (P) Limited Publishers, New Delhi, 2004.

[5]. M. Arivazhagan, R. Kavitha, V.P.Subhasini, Spectrochim. Acta A 130 (2014) 502.

[6]. M. Arivazhagan, K. Sampathkumarr & S. Jeyavijayan, Indian J. Pure & Appl. Phys., 48 (2010) 716.

[7]. S. Jeyavijayan & M. Arivazhagan, Indian J. Pure & Appl. Phys., 48 (2010) 869.

[8]. S. Gunasekaran, R.K. Natarajan, D. Syamala, R. Rathika, Indian J. Pure and Appl. Phys., 44 (2006) 315.

[9]. V. Krishna Kumar & R. John Xavier, J. Chem. Phys., 312 (2005) 227.

[10]. S. Manivel, M. Arivazhagan, E. Palinisamy, G. John James, Elixir vib.spec. 92 (2016) 39112.

[11]. M. Arivazhagan, G. John James, International Journal of scientific research in science, Engg. & Tech. 3 (2017) 434.

[12]. G. Socrates, Infrared and Raman Characteristic Group Frequencies – Tables and Charts, third ed., Wiley, Chichester, 2001.

[13]. G. Ilango, M. Arivazhagan, J. Joseph Prince, V. Balechandran, Ind. J. Pure Appl. Phys., 46 (2008) 698.

[14]. M. Arivazhagan, V.P.Subhasini, R. Kavitha, Spectrochim. Acta A 128 (2014) 527.

[15]. C.H. Choi, M. Kertez, J. Phy. Chem., A101 (1997) 3823.

[16]. S. Gunasekaran, R. Arun Balaji, S. Kumaresan, G. Anand, S. Srinivasan, Can. J. Anal. Sci Spectrosc., 53 (2008) 149.

[17]. D.F.V. Lewis, C. Ioannides, D.V. Parke, Xenobiotica, 24 (1994) 401.

[18]. L. Padmaja, C. Ravikumar, D. Sajan, I.H. Joe, V.S. Jayakumar, G.R. Pettict, O.F. Nielson, J. Raman Spectrosc., 40 (2009) 419.

[19]. C. Ravikumar, I.H. Joe, V.S. Jayakumar, Chem. Phys. Lett., 460 (2008) 552.

[20]. V. Pirnau, O. Chis, N. Oniga, L. Leopold, Szabo, M. Baias, O. Cozar, Vib. Spectros., 48 (2008) 289.

[21]. J.S. Murray, K. Sen, Molecular Electrostatic Potential Concepts and Applications, Elsevier Science B V, Amsterdam, The Netherlands (1996).

[22]. M.A. Palafox, Int J Quant Chem., 77 (2000) 661.

[23]. D.A. Kelinman., Phy. Rev., 126 (1962) 1977

[24]. M. Szafran, A. Komasa, E.B. Aelamska, J. Mol. Struct., (Theochem) 827 (2007) 101.

[25]. C. James, A. Amal Raj, R. Rehunathan, I. Hubest Joe, V.S. Jaya Kumar, J. Raman Spectrosc., 379 (2006) 381.

[26]. Jun-na Liu, Zhi-rang Chen, Shen-fang Yuan, J. Zhejiag Univ. Sci., 6B (2005) 584.

Table 1. Optimized geometrical parameters of m-xylene -alpha, alpha-Diol obtained by DFT/6-31+G and 6-311+G methods and basis set

Bond Length	Values(Å)		Bond Angle	Values (°)		Dihedral Angle	Values (°)	
	B3LYP			B3LYP			B3LYP	
	6-31+ G	6-311+G		6-31+ G	6-311+G		6-31+ G	6-311+G
C1-C2	1.4082	1.405	C2-C1-C6	118.9165	118.8742	C6-C1-C2-C3	-0.2051	-0.2752
C1-C6	1.4027	1.3993	C2-C1-C16	120.1605	120.1818	C6-C1-C2-H7	-179.4233	-179.553
C1-C16	1.5117	1.5105	C6-C1-C16	120.9226	120.9421	C16-C1-C2-C3	179.5641	-179.7803
C2-C3	1.4014	1.3983	C1-C2-C3	121.1761	121.2339	C16-C1-C2-H7	0.3459	0.942
C2-H7	1.0874	1.0836	C1-C2-H7	118.9523	118.8487	C2-C1-C6-C5	-0.3942	-0.3486
C3-C4	1.4095	1.4062	C3-C2-H7	119.867	119.9134	C2-C1-C6-H10	179.8559	179.7563
C3-C11	1.5121	1.5108	C2-C3-C4	119.0841	119.0406	C16-C1-C6-C5	179.8384	179.1525
C4-C5	1.3969	1.3935	C2-C3-C11	120.7098	120.7129	C16-C1-C6-H10	0.0885	-0.7426
C4-H8	1.0858	1.082	C4-C3-C11	120.2036	120.2465	C2-C1-C16-H17	59.5621	64.7904
C5-C6	1.4039	1.4005	C3-C4-C5	120.2532	120.2465	C2-C1-C16-H18	-179.8529	-174.9493
C5-H9	1.0858	1.0822	C3-C4-H8	119.2992	119.2544	C2-C1-C16-C19	-56.1439	-51.2248
C6-H10	1.0871	1.0835	C5-C4-H8	120.4453	120.4966	C6-C1-C16-H17	-120.6734	-114.7042
C11-H12	1.0927	1.0889	C4-C5-C6	120.1447	120.1833	C6-C1-C16-H18	-0.0884	5.556
C11-H13	1.0973	1.0933	C4-C5-H9	119.985	119.96	C6-C1-C16-C19	123.6206	129.2806
C11-O14	1.4713	1.468	C6-C5-H9	119.8691	119.855	C1-C2-C3-C4	0.5852	0.614
O14-H15	0.9793	0.9749	C1-C6-C5	120.4212	120.4171	C1-C2-C3-C11	-179.9914	-179.4252
C16-H17	1.0927	1.089	C1-C6-H10	119.6956	119.722	H7-C2-C3-C4	179.7963	179.8842
C16-H18	1.0975	1.0935	C5-C6-H10	119.8826	119.8608	H7-C2-C3-C11	-0.7803	-0.1551
C16-C19	1.4715	1.4679	C3-C11-H12	111.6293	111.6182	C2-C3-C4-C5	-0.3706	-0.3329
C19-H20	0.9793	0.9749	C3-C11-H13	110.3783	110.2409	C2-C3-C4-H8	179.0814	179.094
			C3-C11-O14	112.8696	112.7912	C11-C3-C4-C5	-179.7969	179.7061
			H12-C11-H13	108.3603	108.2267	C11-C3-C4-H8	-0.345	-0.8669
			H12-C11-O14	103.1448	103.424	C2-C3-C11-H12	120.0298	115.5667

			H13-C11-O14	110.1726	110.2762	C2-C3-C11-H13	-0.552	-4.7459
			C11-O14-H15	110.5533	110.413	C2-C3-C11-O14	-124.3274	-128.4961
			C1-C16-H17	111.7199	111.694	C4-C3-C11-H12	-60.5533	-64.473
			C1-C16-H18	110.3481	110.2089	C4-C3-C11-H13	178.8649	175.2144
			C1-C16-H19	112.918	112.8523	C4-C3-C11-O14	55.0895	51.4642
			H17-C16-H18	108.3315	108.1628	C3-C4-C5-C6	-0.2184	-0.2801
			H17-C16-C19	103.1229	103.4148	C3-C4-C5-H9	-179.8219	-179.8068
			H18-C16-C19	110.1123	110.2411	H8-C4-C5-C6	-179.6641	-179.6998
			C16-C19-H20	110.5625	110.4298	H8-C4-C5-H9	0.7325	0.7734
						C4-C5-C6-C1	0.6068	0.6265
						C4-C5-C6-H10	-179.6437	-179.4785
						H9-C5-C6-C1	-179.7893	-179.8462
						H9-C5-C6-H10	-0.0398	0.0487
						C3-C11-O14-H15	57.0133	57.4061
						H12-C11-O14-H15	177.6314	178.1455
						H13-C11-O14-H15	-66.8755	-66.3246
						C1-C16-C19-H20	-56.3748	-56.7685
						H17-C16-C19-H20	-177.1135	-177.6258
						H18-C16-C19-H20	67.4641	66.9383

Table 2. The observed (FT-IR & FT-Raman) calculated (Unscaled and Scaled) frequencies (cm^{-1})and probable assignments (characterized by TED) m-xylene- alpha, alpha –Diol

S. No	Symm.species C_1	Observed Frequencies		Calculated Values				TED% Among Types Internal Co-ordinates
		FT-IR	FT-Raman	B3LYP/6- 31+ G		B3LYP/6-311+ G		
				Frequencies		Frequencies		
				Unscaled	Scaled	Unscaled	Scaled	
1	A	_	3240	3676	3245	3657	3245	γ O-H (99%)
2	A	3220	_	3629	3224	3656	3224	γ O-H (99%)
3	A	3199	_	3247	3202	3189	3202	γ C-H (99%)
4	A	_	3150	3205	3152	3172	3152	γ C-H (99%)

5	A	_	3062	3182	3067	3161	3067	γ C-H (98%)
6	A	_	2951	3179	2955	3154	2955	γ C-H (97%)
7	A	2947	_	3125	2950	3091	2950	γ CH_2 (96%)
8	A	_	2930	3045	2932	3089	2932	γ CH_2 (96%)
9	A	_	2925	3041	2930	3019	2930	γ CH_2 (95%)
10	A	_	2890	3007	2894	3016	2894	γ CH_2 (94%)
11	A	1601	_	1660	1604	1645	1604	γ C-C (92%)
12	A	_	1511	1639	1513	1626	1513	γ C-C (90%)
13	A	1481	_	1542	1486	1538	1486	γ C-C (91%)
14	A	1460	1463	1536	1464	1534	1464	γ C-C (93%)
15	A	_	1455	1532	1458	1526	1458	γ C-C (90%)
16	A	1448	_	1489	1450	1482	1450	γ C-C (88%)
17	A	1370	_	1437	1375	1416	1375	γ C-C (87%)
18	A	1312	_	1407	1316	1405	1316	γ C-C (86%)
19	A	1288	_	1373	1291	1374	1291	γ C-O (85%)
20	A	1245	1249	1371	1251	1363	1251	γ C-O (82%)
21	A	1239	_	1329	1247	1342	1247	b O-H (78%)
22	A	1209	1210	1293	1217	1316	1217	b O-H (76%)
23	A	_	1190	1254	1196	1284	1196	b C-H (77%)
24	A	1168	_	1225	1173	1216	1173	b C-H (75%)
25	A	1153	_	1213	1157	1198	1157	b C-H (75%)
26	A	1096	_	1185	1099	1194	1099	b C-H(74%)
27	A	1049	_	1156	1051	1186	1051	b CH_2 (72%)
28	A	1010	1015	1128	1023	1123	1023	b CH_2 (71%)
29	A	1000	1001	1057	1008	1029	1008	b CH_2 (73%)
30	A	973	_	1033	979	1021	979	b CH_2 (68%)
31	A	917	_	1027	922	1014	922	b C-C (72%)
32	A	909	910	1026	914	984	914	b C-C (70%)
33	A	889	_	984	892	970	892	b C-C (76%)
34	A	_	820	960	822	964	822	b C-C (70%)
35	A	801	_	949	809	946	809	b C-C (69%)
36	A	793	_	927	800	936	800	b C-O (68%)
37	A	747	750	904	753	904	753	b C-O (67%)
38	A	710	_	819	720	817	720	ω O-H (76%)
39	A	699	_	759	710	768	710	ω O-H (75%)

40	A	–	650	719	662	720	662	ω C-H (73%)
41	A	–	610	628	620	656	620	ω C-H (70%)
42	A	–	590	604	601	586	601	ω C-H (68%)
43	A	588	–	524	600	523	600	ω C-H (66%)
44	A	579	–	454	589	463	589	ω CH_2 (65%)
45	A	–	519	435	530	430	530	ω CH_2 (60%)
46	A	–	450	381	462	382	462	ω C-C (61%)
47	A	439	439	316	449	329	449	ω C-C (63%)
48	A	–	390	284	401	328	401	ω C-C (59%)
49	A	–	280	253	292	288	292	ω C-C (57%)
50	A	–	219	210	229	232	229	ω C-C (56%)
51	A	–	190	191	201	165	201	ω C-O (54%)
52	A	–	163	129	175	129	175	ω C-O (52%)
53	A	–	138	35	148	40	148	ω CH_2 (50%)
54	A	–	130	26	141	34	141	ω CH_2 (45%)

Abbreviations: γ – stretching; b – bending; ω– out-of-plane bending; t – torsion; R – ring; trigd – trigonal deformation; symd – symmetric deformation; asymd – antisymmetric deformation.

Table 3. Hyperpolarizability(β), electric dipole moment (μ) and the polarizability (α_0) at the B3LYP/6-311+G and 6-31+G basis set of m-xylene -alpha, alpha – Diol

Parameters	B3LYP/6-31+ G	B3LYP/6-311+ G
β xxx	-86.7685	-72.241
β xxy	-4.3679	-5.006
β xyy	-13.2763	-8.7099
β yyy	-79.5809	-72.482
β zxx	-7.7530	-4.4500
β xyz	1.1770	0.9177
β zyy	5.8529	13.710
β xzz	4.7079	5.436
β yzz	13.8360	-15.491
β zzz	-19.5039	-16.262
β total	1.0065×10^{-30} esu	1.0041×10^{-30} esu
α xx	-74.2847	-73.5544

α_{xy}	-6.2496	-5.8877
α_{yy}	-60.3136	-60.3306
α_{xz}	0.7455	1.4727
α_{yz}	-1.3163	-0.6797
α_{zz}	-56.3456	-56.3981
α_{0}	0.5326×10^{-30} esu	0.5308×10^{-30} esu
μ_{x}	-1.1934	-1.1749
μ_{y}	1.7286	1.6569
μ_{z}	0.1632	0.1049
μ_{total}	2.1069 Debye	2.0339 Debye

Table 4. The Mulliken charge analyses of m-xylene Alpha, Alpha - Diol calculated by B3LYP method with 6-31+G and 6-311+G basis sets

S.No	**Atoms**	**Mulliken Charges**	
		B3LYP	
		6-31+G	**6-311+G**
1	C_1	0.041054	0.953239
2	C_2	-0.192298	-1.082695
3	C_3	0.200297	1.024442
4	C_4	0.063727	-0.269651
5	C_5	0.091361	0.037363
6	C_6	-0.537739	-0.802865
7	H_7	0.198495	0.239987
8	H_8	0.202803	0.234474
9	H_9	0.179846	0.196466
10	H_{10}	0.178562	0.207077
11	C_{11}	-0.479654	-0.735784
12	H_{12}	0.223839	0.258624
13	H_{13}	0.184101	0.123489
14	O_{14}	-0.516408	-0.390991
15	H_{15}	0.407276	0.325967
16	C_{16}	-0.534854	-0.811914
17	H_{17}	0.222635	0.259381
18	H_{18}	0.181725	0.210599

19	O_{19}	-0.523140	-0.391756
20	H_{20}	0.408374	0.324549

Table 5. Second order perturbation theory analysis of Fock matrix in NBO basic corresponding to the intermolecular bonds of m-xylene alpha, alpha Diol

S.NO	Donor	Acceptor	E(2)	Ej-Ei	F (i,j)
1	$\sigma(C_1\text{-}C_2)$	$\sigma^*(C_2\text{-}C_3)$	3.52	1.27	0.06
2	$\sigma(C_1\text{-}C_6)$	$\sigma^*(C_1\text{-}C_2)$	3.38	1.26	0.058
	π	$\pi^*(C_4\text{-}C_5)$	20.78	0.28	0.068
3	$\sigma(C_1\text{-}C_{16})$	$\sigma^*(C_5\text{-}C_6)$	2.67	1.17	0.05
4	$\sigma(C_2\text{-}C_3)$	$\sigma^*(C_1\text{-}C_2)$	3.57	1.26	0.06
	π	$\pi^*(C_1\text{-}C_6)$	22.51	0.28	0.071
5	$\sigma(C_2\text{-}H_7)$	$\sigma^*(C_3\text{-}C_4)$	4.6	1.08	0.063
6	$\sigma(C_3\text{-}C_4)$	$\sigma^*(C_2\text{-}C_3)$	3.32	1.27	0.058
7	$\sigma(C_3\text{-}C_{11})$	$\sigma^*(C_4\text{-}C_5)$	2.69	1.17	0.05
8	$\sigma(C_4\text{-}C_5)$	$\sigma^*(C_3\text{-}C_{11})$	3.53	1.07	0.055
	π	$\pi^*(C_2\text{-}C_3)$	22.24	0.28	0.07
9	$\sigma(C_4\text{-}H_8)$	$\sigma^*(C_2\text{-}C_3)$	4.76	1.08	0.064
10	$\sigma(C_5\text{-}C_6)$	$\sigma^*(C_1\text{-}C_{16})$	3.46	1.07	0.054
11	$\sigma(C_5\text{-}H_9)$	$\sigma^*(C_3\text{-}C_4)$	3.58	1.09	0.056
12	$\sigma(C_6\text{-}H_{10})$	$\sigma^*(C_1\text{-}C_2)$	4.72	1.09	0.064
13	$\sigma(C_{11}\text{-}H_{12})$	$\sigma^*(O_{14}\text{-}H_{15})$	2.24	0.94	0.041
14	$\sigma(C_{11}\text{-}H_{13})$	$\pi^*(C_2\text{-}C_3)$	0.89	0.56	0.022
15	$\sigma(C_{11}\text{-}O_{14})$	$\sigma^*(C_2\text{-}C_3)$	1.81	1.39	0.045
16	$\sigma(O_{14}\text{-}H_{15})$	$\sigma^*(C_{11}\text{-}H_{12})$	1.84	1.12	0.041
17	$\sigma(C_{16}\text{-}H_{17})$	$\pi^*(C_1\text{-}C_6)$	3.53	0.55	0.043
18	$\sigma(C_{16}\text{-}H_{18})$	$\pi^*(C_1\text{-}C_6)$	0.9	0.56	0.022
19	$\sigma(C_{16}\text{-}O_{19})$	$\sigma^*(C_1\text{-}C_6)$	1.8	1.38	0.045
20	$\sigma(O_{19}\text{-}H_{20})$	$\sigma^*(C_{16}\text{-}H_{17})$	1.84	1.12	0.041
21	$\pi^*(C_1\text{-}C_6)$	$\sigma^*(C_{16}\text{-}H_{17})$	1.44	0.36	0.047
22	$\pi^*(C_2\text{-}C_3)$	$\sigma^*(C_{11}\text{-}H_{12})$	1.41	0.36	0.047

E(2) means energy of hyperconjugative interations
Energy difference between donor and acceptor i and j NBO orbitals.
F(i,j) is the Fock matrix element between i and j NBO orbitals.

Table 6. The Thermodynamic parameters of m-xylene- alpha, alpha Diol calculated by B3LYP method with 6-31+G and 6-311+G basis set

Parameters	Method/Basis Set	
	B3LYP	
	6-31+G	6-311+G
Total Energy E_{total}	110.345	109.964
Heat Capacity (Cv)	35.985	35.992
Entropy (S)	98.993	98.993
Translational	0.889	0.889
Rotational	0.889	0.889
Vibrational	108.568	108.186
Zero Point vibrational Energy	104.21219	103.84281
Rotational Constant(GHZ)		
A	2.34072	2.3449
B	0.79466	0.8016
C	0.63005	0.63083
Dipole Moment		
μ_x	-1.1934	-1.1749
μ_y	1.7286	1.6569
μ_z	0.1632	0.1049
μ_{total}	2.1069	2.0339
Molecular mass	138.06808 amu	138.06808 amu
Rotational Temperature (Kelvin)		
T_1	0.11234	0.11254
T_2	0.03814	0.03847
T_3	0.03024	0.03027

Table 7. Thermodynamic functions of m-xylene- alpha, alpha-Diol calculated at B3LYP/ 6-311+G method

S.No	Temperature	Enthalpy (E)	Heat Capacity (Cv)	Entropy (S)
		Kcal/Mol	Cal/Mol-Kelvin	Cal/Mol-Kelvin
1	100	104.921	15.454	71.005
2	200	106.96	25.375	86.12
3	300	110.03	36.199	99.229
4	400	114.2	47.04	111.72

5	500	119.391	56.497	123.708

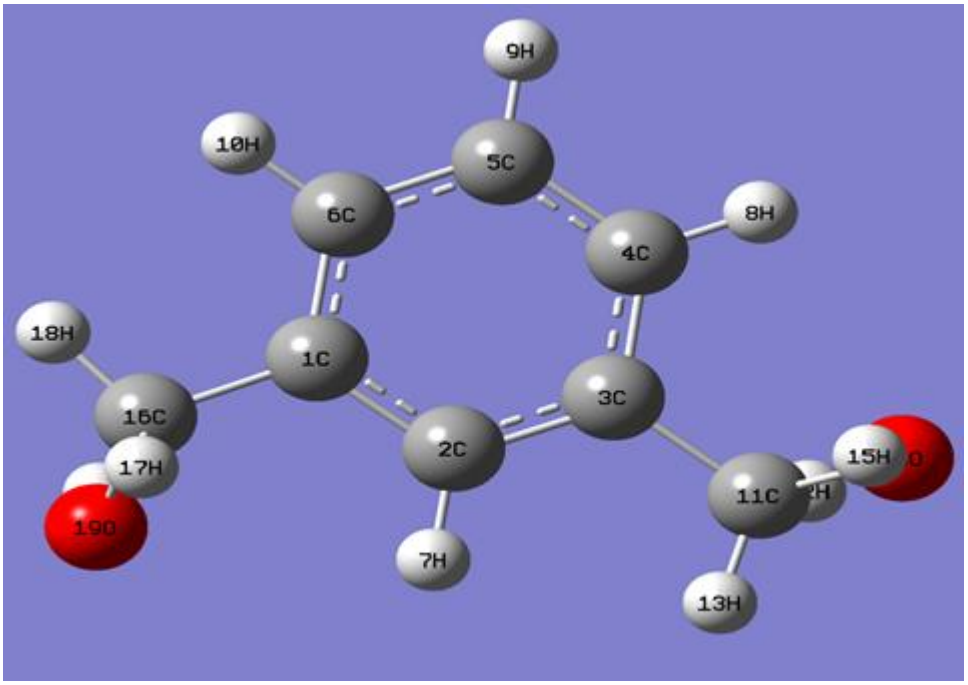

Figure 1. Optimized molecular structure of m-xylene alpha, alpha – Diol

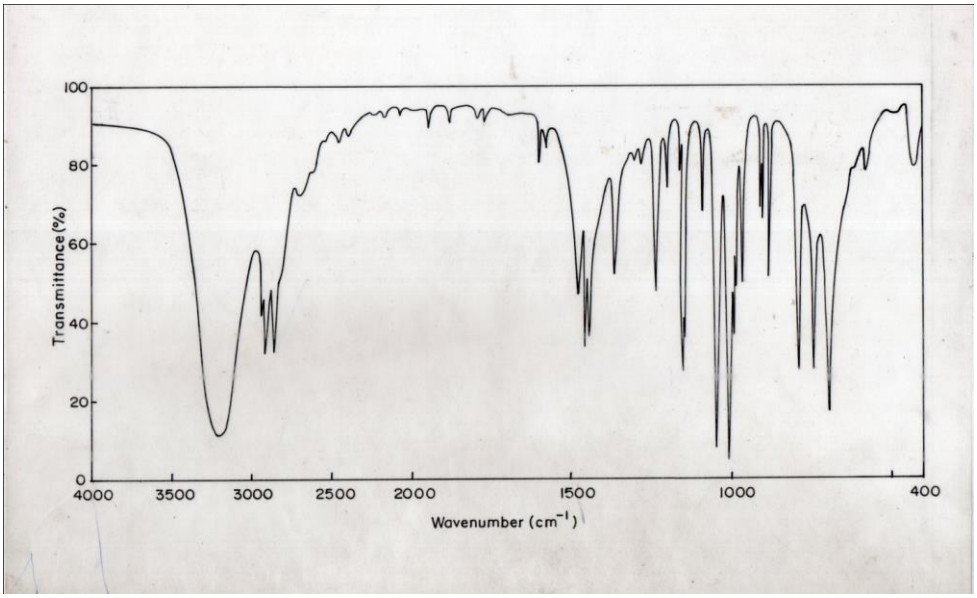

Figure 2. FT-IR Spectrum of m-xylene alpha, alpha - Diol

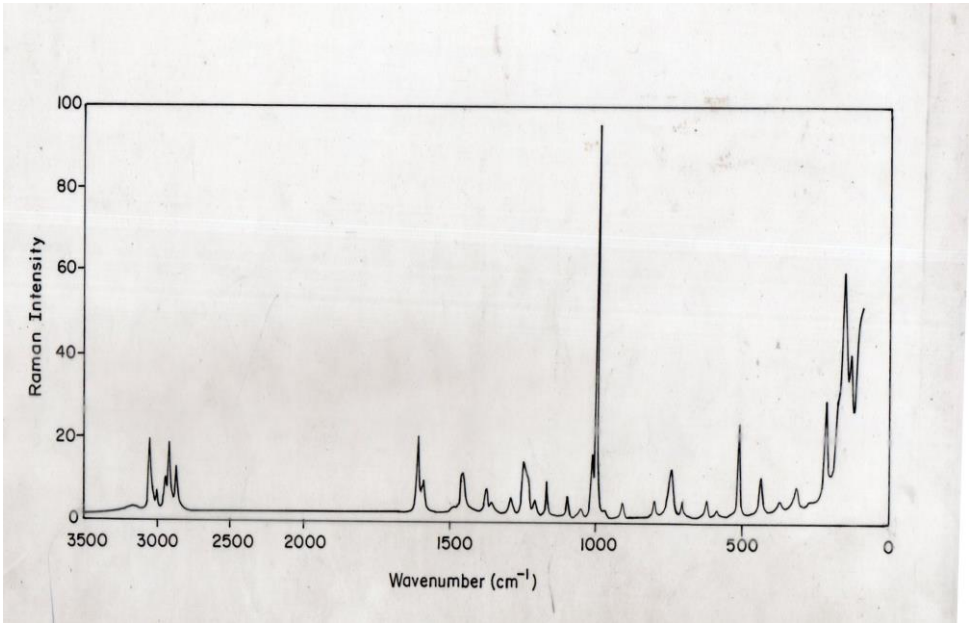

Figure 3. FT-Raman Spectrum of m-xylene alpha, alpha – Diol

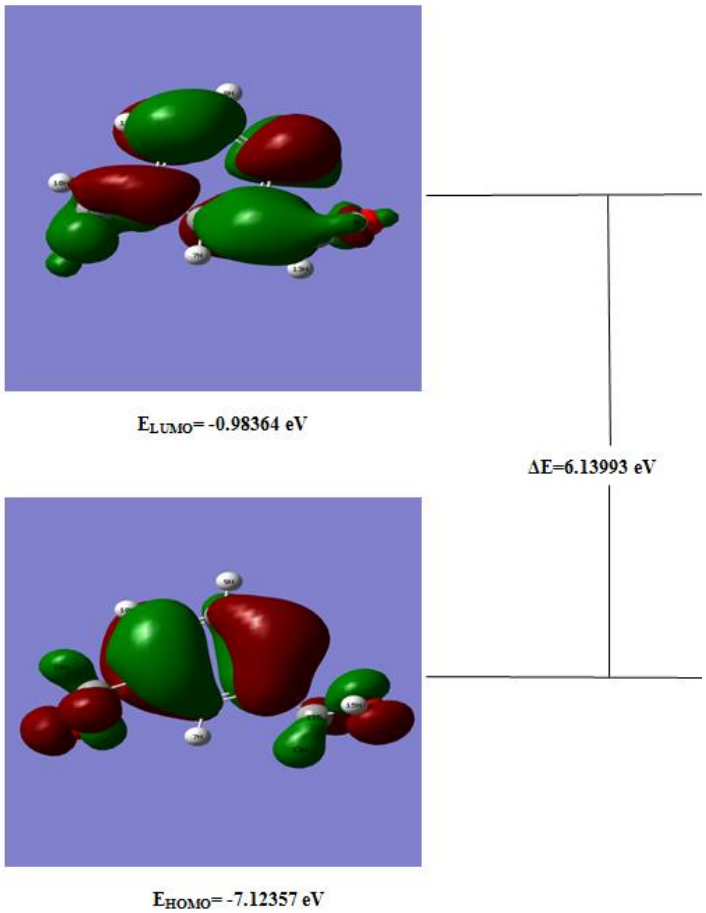

Figure. 4 HOMO and LUMO plot of m-xylene alpha, alpha –Diol

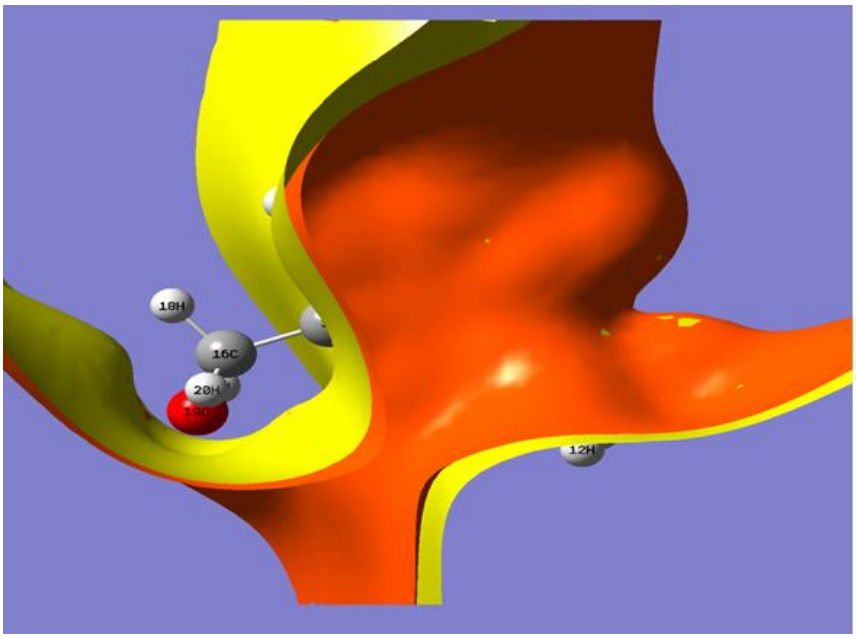

Figure. 5 Molecular Electrostatic Potential (MEP) map of m-xylene -alpha, alpha –Diol

Figure 6. Plot of Mulliken's atomic charges of m-xylene alpha, alpha - Diol

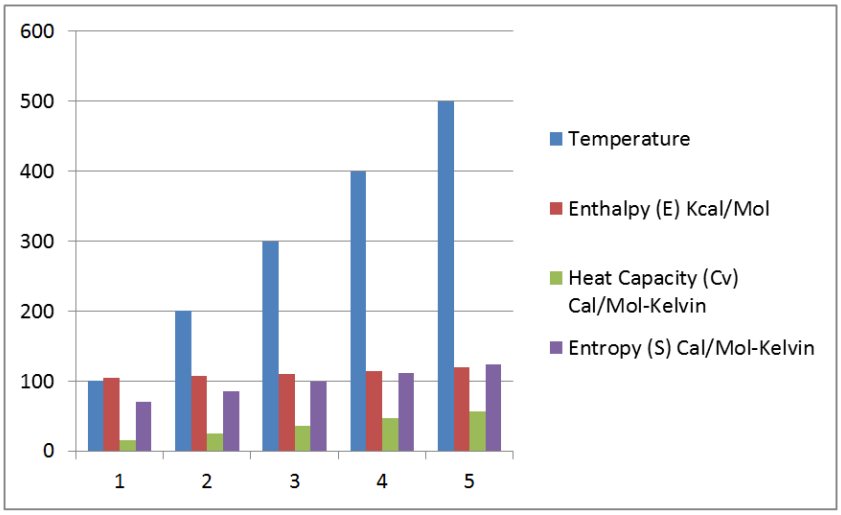

Figure 7. Correlation graphic relation between Heat capacity (Cv), Entropy (S), Enthalpy (E) of m-xylene alpha, alpha-Diol